Semianalytical Solution for CO 2 Leakage through an Abandoned Well

ARTICLE *in* ENVIRONMENTAL SCIENCE AND TECHNOLOGY · FEBRUARY 2005

Impact Factor: 5.33 · DOI: 10.1021/es035338i · Source: PubMed

4 AUTHORS, INCLUDING:

Stefan Bachu
Alberta Innovates
169 PUBLICATIONS **6,061** CITATIONS
SEE PROFILE

Helge K. Dahle
University of Bergen
71 PUBLICATIONS **1,558** CITATIONS
SEE PROFILE

Environ. Sci. Technol. **2005**, *39,* 602−611

Semianalytical Solution for CO_2 Leakage through an Abandoned Well

JAN MARTIN NORDBOTTEN,[†] MICHAEL A. CELIA,*[,‡] STEFAN BACHU,[§] AND HELGE K. DAHLE[†]

Department of Mathematics, University of Bergen, Bergen, 5020, Norway, Environmental Engineering and Water Resources Program, Department of Civil and Environmental Engineering, Princeton University, Princeton, New Jersey 08544, and Alberta Geological Survey, Alberta Energy and Utilities Board, Edmonton, Alberta, T6B 2X3 Canada

Capture and subsequent injection of carbon dioxide into deep geological formations is being considered as a means to reduce anthropogenic emissions of CO_2 to the atmosphere. If such a strategy is to be successful, the injected CO_2 must remain within the injection formation for long periods of time, at least several hundred years. Because mature continental sedimentary basins have a century-long history of oil and gas exploration and production, they are characterized by large numbers of existing oil and gas wells. For example, more than 1 million such wells have been drilled in the state of Texas in the United States. These existing wells represent potential leakage pathways for injected CO_2. To analyze leakage potential, modeling tools are needed that predict leakage rates and patterns in systems with injection and potentially leaky wells. A new semianalytical solution framework allows simple and efficient prediction of leakage rates for the case of injection of supercritical CO_2 into a brine-saturated deep aquifer. The solution predicts the extent of the injected CO_2 plume, provides leakage rates through an abandoned well located at an arbitrary distance from the injection well, and estimates the CO_2 plume extent in the overlying aquifer into which the fluid leaks. Comparison to results from a numerical multiphase flow simulator show excellent agreement. Example calculations show the importance of outer boundary conditions, the influence of both density and viscosity contrasts in the resulting solutions, and the potential importance of local upconing around the leaky well. While several important limiting assumptions are required, the new semianalytical solution provides a simple and efficient procedure for estimation of CO_2 leakage for problems involving one injection well, one leaky well, and multiple aquifers separated by impermeable aquitards.

Introduction

Atmospheric concentrations of greenhouse gases, such as carbon dioxide (CO_2) and methane (CH_4), have increased since the industrial revolution to the point that significant climate warming and weather changes have been attributed to anthropogenic activity. A major challenge in mitigating anthropogenic effects on climate change is the reduction of CO_2 emissions to the atmosphere. Such reduction may be achieved by (i) lowering the energy intensity of the economy by increasing the efficiency of primary energy conversion and end use, including conserving energy; (ii) lowering the carbon intensity of the energy system by substituting lower carbon or carbon-free energy sources for the current sources; and (iii) artificially increasing the capacity and capture rate of carbon sinks (*1*, *2*). Since fossil fuels are likely to remain a major component of world's energy supply for at least this century (*3*, *4*), it is unlikely that a reduction in net CO_2 emissions into the atmosphere can be achieved only through energy conservation and efficiency. Thus, enhancement of CO_2 sinks is likely to play a significant role in reducing CO_2 emissions into the atmosphere.

One promising option for CO_2 mitigation is capture and subsequent injection of CO_2 into deep geological formations. Such an option is attractive because the technology for injection already exists, and it has already been applied for enhanced oil recovery, acid gas disposal, and deep disposal of hazardous wastes (e.g., ref *5*−*9*). However, none of these activities approaches the scale involved in CO_2 injection, where a substantial fraction of the 25 Gt (gigaton) of CO_2 produced per year needs to be sequestered away from the atmosphere. Many issues need to be addressed before large-scale implementation of CO_2 geological sequestration, with an important one being the potential for CO_2 leakage (*10*, *11*). Because free-phase CO_2 will always be lighter than formation water (*2*), the potential for upward leakage is enhanced by CO_2 buoyancy. Leakage may occur through natural geological features such as faults or fractures, perhaps enhanced by fluid over-pressurization associated with the injection, or it may occur through human-created pathways such as existing wells (*11*). It is important to estimate the potential for CO_2 leakage from injection formations into overlying units because of the need to (i) protect existing and potential energy and mineral resources; (ii) protect shallow groundwater resources and soils; and (iii) avoid significant leakage back into the atmosphere, with possible effects on vegetation, near-surface ecosystems, and the carbon balance (*11*, *12*). Leakage of CO_2 back into the atmosphere has been recognized in the context of the global carbon balance as being unavoidable in the long term but acceptable if it is small enough. Recent global analyses indicate maximum acceptable leakage rates between 0.01% (*13*) and 1.0% (*14*) leakage per year, where the percent fraction is defined as the volume leaked globally in that year as compared to total cumulative volume stored. Leakage rates below these estimated rates are required to maintain atmospheric levels of CO_2 within the targets suggested by the International Panel on Climate Change (*15*).

Possible leakage of CO_2 through existing wells appears to be especially important in mature sedimentary basins that have been intensively explored and exploited for hydrocarbon production, such as those in North America. For example, more than 350 000 oil and gas wells have been drilled to date in the province of Alberta, Canada, while more than 1 000 000 wells have been drilled in the state of Texas in the United States. Both of these locations are major energy producers in North America. The density of wells is particularly high in producing areas, reaching, for example, more than 10 wells/km^2 in certain areas in Alberta (*16*). A large number of wells are abandoned, approaching or even passing 50% of all wells, depending on basin maturity. Well completion and abandonment practices have evolved in time, from simply walking

* Corresponding author phone: (609)258-5425; fax: (609)258-2799; e-mail: celia@princeton.edu.
[†] University of Bergen.
[‡] Princeton University.
[§] Alberta Energy and Utilities Board.

10.1021/es035338i CCC: $30.25

Published on Web 12/13/2004

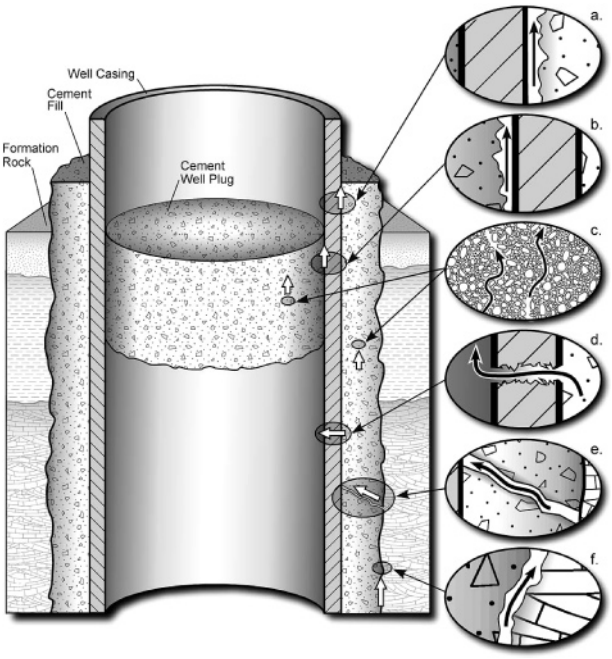

FIGURE 1. Potential pathways for leakage along an abandoned well, including flow along material interfaces (a, b, f) and through well cements and casing (c, d, e).

away in the 19th century to currently very stringent procedures imposed by regulatory agencies. Considering the extreme variability in field practices, regulatory requirements, material quality, and subsurface conditions, and the fact that the injected CO_2 is supposed to remain underground for several centuries, during which even wells drilled and abandoned by today's standards are likely to degrade, the issue of CO_2 leakage from the injection formation requires special attention.

If CO_2 is injected into a deep saline aquifer, a free-phase CO_2 plume will form that will expand during injection and afterward will migrate afterward up-dip along the bedding. While CO_2 is soluble in formation water, its solubility limit is about 4 vol %, and the waters into which it will dissolve in the short to intermediate term are restricted to the residual water behind the infiltrating front. At longer times, on the order of hundreds to a few thousand years, larger-scale dissolution and miscible transport become important, perhaps with enhanced mixing in the aqueous phase due to gravity instabilities (*17*). During the short to intermediate time scales, the CO_2 plume may travel a distance of several kilometers (*18*, *19*) and come into contact along its path with wells that penetrate the injection formation. If the wells are degraded prior to or during their contact with CO_2, then CO_2 may leak upward along several possible paths: between cement and formation rock, through the cement, between cement and casing (if the well was cased), through the cylindrical space within the casing if the casing is corroded, and through cement plugs if they are damaged or degraded (*11*), see Figure 1.

The issue of potential leakage of hazardous wastes through wells into shallow groundwater aquifers has been identified by regulatory agencies and researchers more than 2 decades ago (see ref *20* and references therein). Several recent studies have attempted to identify CO_2 leaks from both natural reservoirs and from enhanced oil recovery operations (e.g., ref *21*), and others have attempted to study the ultimate fate of the CO_2 plume within the injection formation (e.g., refs *18* and *22*−*25*). Lindeberg (*23*) simulated CO_2 leakage from a high-permeability aquifer, characteristic of the North Sea basin, through a fracture at the outer boundary of a horizontal aquifer by removing CO_2 from the system once it reaches a distance of 8000 m from the injection well. Saripalli and McGrail (*25*) considered the issue of CO_2 leakage through a fracture and assessed the flow rate in laminar flow between the fracture planes as a function of CO_2 buoyancy and viscosity and fracture aperture, width, and length. No assessment exists to date of the leakage potential through wells.

In a recent study (*20*), we developed an analytical solution for the problem of aqueous-fluid injection and leakage involving an arbitrary number of injection wells, an arbitrary number of leaky abandoned wells, and an arbitrary number of geological layers. The solution allowed us to calculate and assess cross-formational leakage and ultimately leakage to the land surface. In the present study, we build on that earlier work to develop a solution for the case of CO_2 injection that includes leakage through an abandoned well. The resulting semianalytical solution procedure provides estimates for cross-formational leakage rates for both CO_2 and the resident brine in the formation. These semianalytical solutions are very efficient and allow for fast calculations, thereby offering the possibility to perform large-scale analyses with many statistical realizations of the system. This study is part of our overall research program into possible leakage mechanisms for CO_2 and estimation of associated leakage rates for CO_2 injection scenarios into deep aquifers.

Fluid Properties of CO_2 and Brine

At normal atmospheric conditions, CO_2 is a thermodynamically very stable gas heavier than air (CO_2 density at standard conditions is 1.872 kg/m^3). For temperatures greater than T_c = 31.1 °C and pressures greater than P_c = 7.38 MPa (critical point), CO_2 is in a supercritical state with density that increases, depending on pressure and temperature, from 150 to >800 kg/m^3 for the temperature and pressure conditions found in sedimentary basins (*2*). For conditions typical of sedimentary basins, viscosity of the CO_2 is between 5 and 40 times lower than viscosity of the resident brine (*19*). Density and viscosity as a function of pressure and temperature are shown in Figure 2a,b. Notice that all values of CO_2 density are below the density of the background brine, so the CO_2 will always experience buoyancy forces. Notice also that the compressibility, as measured by the change in density with pressure, is relatively mild for most values of temperature and pressure in the supercritical range, with the exception being for values near the critical point. We return to this point later in the paper.

Model for CO_2 Injection and Leakage in Wells

In the present work, we are interested in the problem of injection of dense-phase CO_2 into a deep saline aquifer, with inclusion of possible leakage through an abandoned well in the vicinity of the injection well. The CO_2 is assumed to be liquid or supercritical, with density that is large relative to the gas phase but still less than the density of brine. For this problem, there are two different time scales associated with the injection. The first is the transient pressure pulse that moves away from the injection well, through the aqueous fluid. By analogy to the single-fluid work of ref *20*, this may be represented by an outer boundary that expands in proportion to $\sqrt{t}$. This pressure pulse may lead to initial brine leakage out of the formation, as in the single-fluid case. The second time scale corresponds to the front of advancing CO_2. Blunt and King (*26*) showed that this front also moves as $\sqrt{t}$, and Nordbotten et al. (*19*) showed that for most practical cases of CO_2 injection the shape of the CO_2 plume is determined primarily by the viscosity ratio of the two fluids. The role of gravity is discussed below.

CO_2 Injection Solution. If CO_2 transport is dominated by viscous forces, then a simple solution to the radial Buckley−

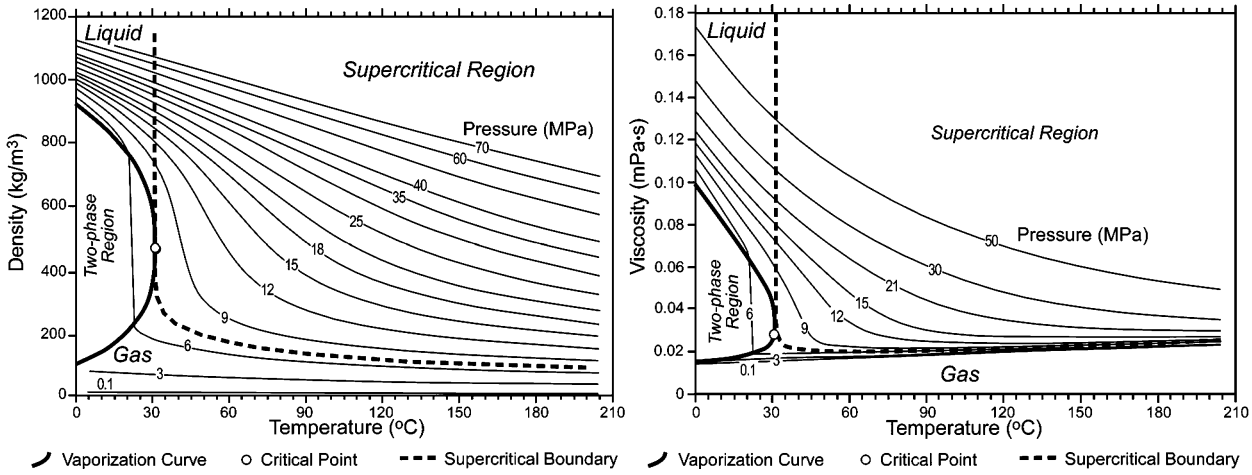

FIGURE 2. CO_2 density and viscosity as functions of pressure and temperature.

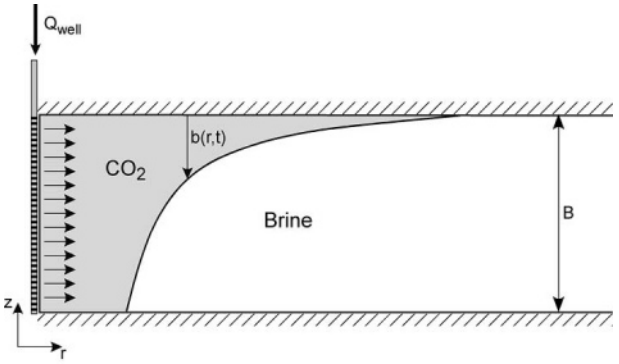

FIGURE 3. Schematic of sharp-interface representation of injected CO_2 plume.

Leverett equation may be used to describe the saturation evolution with radial distance and time (see, for example, refs *26* and *27*). If we represent the CO_2 as being vertically segregated due to buoyancy, so that the fastest "viscous fingers" always occur along the top of the formation, then we may represent the solution schematically as in Figure 3, where the CO_2 and brine are separated by a sharp interface. The analytical solution may be written as (*19*, *26*):

$$\frac{b(r,t)}{B} = \frac{1}{\lambda_c - \lambda_w}\left[\sqrt{\frac{\lambda_c \lambda_w V(t)}{\varphi(1 - S_{res})\pi B r^2}} - \lambda_w\right] \qquad (1)$$

In eq 1, $V(t)$ is the cumulative volume injected up to time t [L^3], the phase mobility λ_α is defined as the ratio of relative permeability to fluid viscosity, $\lambda_\alpha = k_{r\alpha}/\mu_\alpha$ [M^{-1} LT], where α identifies each fluid, with α = w for water (brine) and α = c for CO_2, φ is porosity [L^3/L^3], S_{res} is the residual CO_2 saturation behind the invading front [L^3/L^3]. r is radial distance from the injection well [L], t is time [T], B is the total thickness of the aquifer [L], and b is the thickness of the CO_2 plume [L] as a function of r and t. When evaluating eq 1, b is set equal to zero when the left side of the equation is negative, and b is set equal to B when the left side exceeds one. When $\lambda_c = \lambda_w$, the CO_2 invades with a simple cylindrical shape, with the volume corresponding to $V(t)$. Note that eq 1 is based on an assumption that vertical equilibrium (*28*, *29*) applies to the overall flow system so that pressure is a function of radial distance and time. The equation also neglects capillary pressure and assumes constant density for each fluid within the formation.

While the assumptions involved in the derivation of this equation appear to be significant, we provide the following justification. In ref *19*, we have analyzed the system through energy arguments and through comparisons to numerical simulations based on the industry-standard simulator Eclipse (*30*). In regard to explicit inclusion of gravity in the solution, we find that applicability of eq 1 is determined by the dimensionless grouping Γ, defined by (*19*, *31*):

$$\Gamma = \frac{2\pi(\rho_b - \rho_c)gk\lambda_w B^2}{Q} \qquad (2)$$

where Q is the injection rate [L^3 T^{-1}], g is the gravitational constant [L T^{-2}], k is the intrinsic permeability of the formation [L^2], and ρ_b and ρ_c are densities of brine and CO_2, respectively [ML^{-3}]. When Γ <0.5, eq 1 gives very accurate solutions for both pressure and saturation distributions as a function of radial distance and time, when compared to numerical solutions from Eclipse. The solutions also scale as r^2/t. We have analyzed CO_2 injection scenarios across a range of expected parameter values, for formations at different depths and with different geothermal gradients, and found that Γ remains below 0.5 and is usually well below that value for most practical CO_2 injection scenarios. Furthermore, the numerical simulations show that the fastest flowing part of the CO_2 front is driven to the top of the formation by buoyancy, even when Γ is small, and that the buoyant drive tends to smooth the front and vertically segregate viscous instabilities. More details of this analysis can be found in ref *19*.

We have also studied the assumption of constant density and viscosity and reported our results in ref *19*. For most ranges of temperature and pressure, the change of density with pressure is around 2×10^{-5} [kg m^{-3} Pa^{-1}] and viscosity changes are on the order of 5×10^{-9} [Pa·s/Pa] (see Figure 2). When these values are used in a full numerical simulation (for example, using Eclipse), the computed solution changes by less than 5%. The only exception to this is in the supercritical region near the critical point, which corresponds to warm (high geothermal gradient) sedimentary basins. There the changes in density and viscosity, per change in pressure, are about an order of magnitude higher, and the resulting solutions showed a small shift in location of the front but the front shape remains well represented. Overall, based on the results in ref *19*, we concluded that the assumption of constant fluid properties within a given formation appears to be reasonable and that, for many practical CO_2 injection problems, eq 1 provides a good model for plume evolution. We provide additional numerical testing in the Results section of this paper.

Leakage through an Abandoned Well. When injection takes place in the vicinity of one or more abandoned wells, leakage may occur through those abandoned wells, with fluid

migrating from the formation into which injection takes place to other formations and perhaps to the land surface. For the single-fluid, aqueous-flow case treated in ref *20*, the equations that govern the multiple well system were linear so, with appropriate approximation of the convolution integrals associated with leakage, a set of linear algebraic equations resulted from which leakage rates were calculated. In the two-fluid flow problem, the inherent nonlinearities preclude direct use of superposition; therefore, alternate formulations must be developed.

For the two-fluid case, we will extend the overall approach of ref *20* to include two-fluid flow in the injection formation, in the leaky well, and from the leaky well into an overlying permeable formation. Fluid potential differences between successive aquifers cause flows in the leaky well. These leakage flows in turn cause local drawdowns in the injection aquifer and local pressure increases in the aquifer above, thereby providing coupling between leakage rates and pressures in the affected aquifers. In this paper, we develop a solution methodology for two deep aquifers separated by an intervening aquiclude, with one injection well and one leaky well.

We consider cases for which leakage pathways are through regions of degraded well cements or through very thin annular openings or fractures (see Figure 1), such that the multiphase version of Darcy's law is applicable. For flow between layer l and its neighbor layer, l+1, the expression for volumetric flow rate is

$$Q_\alpha = -(\pi {r_{\text{well}}}^2) k_{\text{well}} \lambda_\alpha \left(\frac{p_{l+1} - p_l}{D_{l+}} + \rho_\alpha g \right) \tag{3}$$

In eq 3, Q_α is the volumetric flow (leakage) rate of fluid α in the well [$L^3\ T^{-1}$]; r_{well} is the effective well radius [L], k_{well} denotes the effective intrinsic permeability of the leaky well [L^2]; p_{l+1} and p_l are the pressures in the upper and lower aquifers, respectively; and D_{l+} is the vertical distance (aquitard thickness) between the two aquifers [L]. The mobilities λ_α in the well are functions of the saturation, which will be discussed below. Because the flow in the well is vertical, buoyancy is included explicitly in eq 3.

Flows through the abandoned well induce a kind of upconing of more dense brine, thereby thinning the CO_2 layer at the leaky well and producing an extended period of two-fluid flow in the well. This is analogous to upconing of saltwater in coastal aquifers (see, e.g., ref *32*). All else being equal, the saturation in the well depends on the local saturation around the well and the leakage rate, with higher leakage rates producing more upconing and therefore lower saturations of CO_2. A simple way to capture this is to assign a maximum CO_2 layer thickness at the well, above which flow of brine in the well, associated with the upconing behavior, is precluded by the presence of CO_2. Below this maximum thickness the saturation in the well is taken to vary linearly in proportion to the thickness of the CO_2 layer. Because the upconing depends on the flow rate, we expect the maximum thickness to depend on the leakage rate. Let the maximum thickness be denoted by $b_{\max}$. Then the saturation in the leaky well is given by the following equation:

$$S_{cl+} = \begin{cases} 0 & b_{\text{well}} = 0 \\ \dfrac{b_{\text{well}}}{b_{\max}} & 0 < b_{\text{well}} < b_{\max} \\ 1 & b_{\text{well}} > b_{\max} \end{cases} \tag{4}$$

where S_{cl+} denotes volumetric saturation of CO_2 [L^0] in the leaky well between layers l and l+1, and b_{well} denotes the thickness of the CO_2 plume at the leaky well. We discuss the choice of the parameter $b_{\max}$ in the Results section. Given the saturation in this portion of the leaky well, we may calculate the mobilities and therefore determine the flow rates, based on eq 3.

Transport of Leaked Fluids. Consider the early-time situation when the injected CO_2 has not reached an abandoned well but the pressure pulse has, such that brine may begin to leak. The presence of CO_2 in the domain causes changes to the vertically averaged fluid mobility λ (see after eq 6 for definition). The initial region of modified mobility has radial symmetry with respect to the injection well, but it loses symmetry when the leaking well activates. It also fails to have symmetry with respect to the abandoned well. Because we wish to maintain radial symmetry in the fundamental solutions, we make the following approximations. First, we will always assume radial symmetry of the CO_2 plume with respect to the injection well. Our reasoning is that the injection well is the dominant feature of the system and to first order it controls the pressure and fluid movements. We therefore view leaking wells as small perturbations with respect to the injection process. In addition, because we are ultimately interested in systems with hundreds of potentially leaking wells, with locations that are essentially random in space (see, for example, ref *16*), the effects of leakage will tend to be distributed uniformly in space; therefore, overall symmetry of the injection plume is likely. When considering the solution for pressure reductions, or drawdowns due to flow in the leaking well, the argument is a bit more complex. One of the complicating features is the existence of a CO_2 plume that is symmetric with respect to the injection well but not with respect to the leaky well. That CO_2 plume causes an inhomogeneous mobility function that is not symmetric with respect to the leaky well. To deal with the spatial variability of mobility, we choose to compute two different solutions for the drawdown around a leaky abandoned well. Each imposes radial symmetry, with one providing an estimate for an upper bound on the solution, and the other providing a lower bound. Mathematically, the bounds are based on the following generated mobility fields:

$$\lambda^{\text{L}}(r) = \max_\theta \lambda(r,\theta)$$

$$\lambda^{\text{U}}(r) = \min_\theta \lambda(r,\theta) \tag{5}$$

In eq 5 superscripts L and U denote lower and upper bounds, respectively, for drawdown at the leaky well, and θ is the angular coordinate direction in the radial coordinate system centered at the abandoned well. We note that these bounds are not strict in the mathematical sense, but they do provide reasonable heuristic bounds for the well leakage problem. Figure 4 shows the symmetrization region associated with these bounds.

The drawdown calculation is continued after the CO_2 front arrives at the abandoned well. However, now the point-wise disappearance (flow) of CO_2 from the injection formation needs to be accounted for. To maintain radial symmetry, we take the calculated amount of leaked CO_2 and remove it uniformly from the outside edge of the CO_2 plume, over the entire circumference of the circle of injected CO_2. Because the amount of leakage out of any single well is typically quite small, as compared to the injection rate, this turns out in practice to be a reasonable assumption. The case for this assumption is strengthened when we consider that our ultimate goal is to simulate simultaneous leakage through tens to hundreds of abandoned wells, scattered throughout the domain. In that case, the spatial distribution of wells implies a more uniform extraction of CO_2 through leakage, resulting in a less distorted CO_2 injection plume.

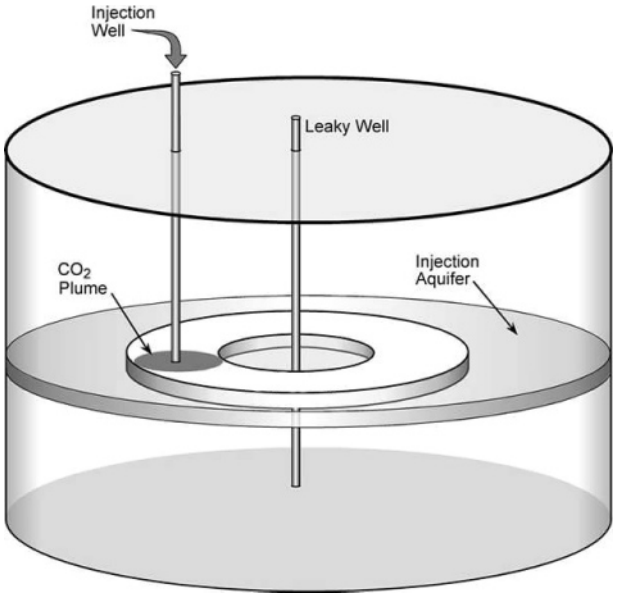

FIGURE 4. Schematic showing region associated with the upper and lower bounds for drawdown effects at the leaky well.

Finally, let us consider how leaking CO_2 flows into adjacent permeable units (note that brine flow, prior to arrival of CO_2, is identical to the approach described in ref *20*). The solution procedure (see the complete algorithm below) provides pressure values at the location of the leaky well, one for each permeable formation in a layered system. From this information volumetric fluxes of CO_2 are calculated. Given a CO_2 flux into a permeable formation, the analytical procedure described above (for the injection well) is again applied to determine the extent and shape of the CO_2 plume in that formation.

Overall Algorithm

As opposed to the one-fluid flow case, for two-fluid flow we cannot avoid time-stepping because we need to explicitly advance the CO_2 front. The overall algorithm that we adopt is based on the following IMPES (IMplicit Pressure Explicit Saturation)-type of procedure:

(i) Solve the system of pressure equations based on the injection solution, as well as the leakage solutions, using well saturations from the previous time step.

(ii) From the pressure solutions, determine leakage fluxes, transport fluids based on these fluxes, and update the saturations in the leaky well.

(iii) Repeat the procedure at the next time level.

Pressure Equations. We begin by defining a fundamental pressure solution $G(\mathbf{x},t)$ as the solution to the following vertically averaged equation for pressure in the formation, derived from summation of the two phase equations and the assumption of incompressible fluids:

$$-kB\nabla(\lambda\nabla G) = I\delta(\boldsymbol{x} - \boldsymbol{x}_{\text{well}}) \tag{6}$$

In eq 6, $\lambda(r)$ denotes vertically averaged mobility ($\lambda = (b\lambda_c + (B-b)\lambda_w)/B$) [$M^{-1}$ LT], G denotes the fundamental solution to the equation, taken to have units of pressure [$ML^{-1}T^{-2}$]; I denotes a unit value with dimensions [L^3T^{-1}]; and δ is the Dirac delta function centered at the point $\boldsymbol{x}_{\text{well}} = (x_{\text{well}}, y_{\text{well}})$ [L^{-2}]. Because of the simple mathematical form of the plume shape, the solution G can be obtained analytically. We can then use this fundamental solution to write the general expression for pressure changes due to injection and leakage. First we observe that for any arbitrary volumetric flow rate through a source or sink (a well) located at $\boldsymbol{x} = \boldsymbol{x}_{\text{well}}$, the pressure solution takes the form of

$$\bar{p}(\boldsymbol{x},t) - \bar{p}_{\text{init}} = \int_0^t \frac{\partial Q_{\text{well}}(t')}{\partial t} G(\boldsymbol{x}, t-t')\, dt' \equiv \frac{\partial Q_{\text{well}}}{\partial t} * G \tag{7}$$

where * denotes convolution integral, subscript init implies initial condition (taken to be constant), and the overbar denotes an average pressure taken to be constant in the vertical (over the formation thickness B). Now consider the case of one injection well and one potentially leaky abandoned well. Assume the injection well has a constant injection rate. Then, taking into account the possible (time varying) leakage through the abandoned well, we have the following equation for pressure within the injection formation:

$$\bar{p}(\boldsymbol{x},t) - \bar{p}_{\text{init}} = Q_{\text{inj}} G_{\text{inj}}(\boldsymbol{x},t;b) + \left(\frac{\partial Q_{\text{leak}}}{\partial t} * G_{\text{leak}}\right)(\boldsymbol{x},t;b) \tag{8}$$

In eq 8, the fundamental solutions G are written to explicitly indicate their dependence on the CO_2 plume (dependence on b) because of the important dependence on mobility.

On the basis of our earlier work (see ref *20*), the convolution integral is approximated using a Heaviside step function to represent the leakage flux Q_{leak}. The step function has magnitude $Q_{\text{leak}}(t)$ and is taken to change from zero to $Q_{\text{leak}}(t)$ at time $t' = (1-\gamma)t$. In the one-fluid case (*20*), numerical testing indicated that a good choice for the parameter γ was $\gamma = 0.92$. The reason this approximation works so well is that the leakage flux, as a function of time, has a self-similar form; therefore, this simple evaluation preserves the proper integral value. When this step function is used, the time derivative in the convolution integral becomes a Dirac delta function, so the convolution integral is reduced to an evaluation of the fundamental solution G at a single point γt in time, while Q_{leak} is evaluated at the current time t. In the two-fluid case, we have two distinct time scales, one associated with the initial (single-phase) pressure pulse that defines the outer radius and a second one associated with the CO_2 saturation front. Therefore, we use a sum of two step-functions, the first applied to the initial time period (pressure pulse) and the second applied to the time following arrival of the CO_2 saturation front. By analogy to the one-fluid case, we choose the first step using $\gamma_1 = 0.92$. For the second time period we have used $\gamma_2 = 1$, which has given good solutions when compared to full numerical simulations.

These equations may be combined to yield a model for leakage of CO_2 from a formation into which it is injected, to overlying formations, each separated by an impervious aquitard or aquiclude. If the leakage rate expression of eq 3 is substituted into eq 8 and the Heaviside step approximation is applied, then we have the following equation for pressure in aquifer number l:

$$\begin{aligned}\bar{p}_l(\boldsymbol{x},t) - \bar{p}_{l,\text{init}} = {} & Q_{\text{inj}} G_{\text{inj},l}(\boldsymbol{x},t;b_l) + \\ & \sum_{\alpha=c,w}\left[\pi r_{\text{leak}}^2 k_{l+}\lambda_{\alpha,\text{leak},l+} \times \left(\frac{\bar{p}_{\text{leak},l+1} - \bar{p}_{\text{leak},l}}{D_{l+}} + \rho_\alpha g\right)\right] G_{\text{leak},l}(\boldsymbol{x},\hat{\gamma}t;b_l) - \\ & \sum_{\alpha=c,w}\left[\pi r_{\text{leak}}^2 k_{l-}\lambda_{\alpha,\text{leak},l-} \times \left(\frac{\bar{p}_{\text{leak},l} - \bar{p}_{\text{leak},l-1}}{D_{l-}} + \rho_\alpha g\right)\right] G_{\text{leak},l}(\boldsymbol{x},\hat{\gamma}t;b_l)\end{aligned} \tag{9}$$

In eq 9, the value of $\hat{\gamma}$ is taken to be equal to γ_1 until the CO_2 plume arrives at the leaky well, after which it is set to γ_2. To derive the algebraic equations that are actually solved for

pressure, we evaluate eq 9 at the abandoned well location, in each aquifer, and solve for the pressures at the wells. Because mobilities (λ) are functions of fluid saturation, we evaluate the nonlinear coefficients in the leakage terms using saturation values from the previous time step. If superscript n denotes discrete time level, then the equation for pressure at the time step $n + 1$, evaluated at the abandoned well, is written as

$$\bar{p}_l(\boldsymbol{x}_{\text{leak}}, t^{n+1}) - \bar{p}_{l,\text{init}} \equiv \bar{p}^{n+1}_{\text{leak},l} - \bar{p}_{l,\text{init}} = Q_{\text{inj}} G_{\text{inj},l}(\boldsymbol{x}_{\text{leak}}, t^{n+1}; b_l^n) + \sum_{\alpha=c,w} \left[\pi r^2_{\text{leak}} k_{l+} \lambda^n_{\alpha,\text{leak},l+} \times \left(\frac{\bar{p}^{n+1}_{\text{leak},l+1} - \bar{p}^{n+1}_{\text{leak},l}}{D_{l+}} + \rho_\alpha g \right) \right] G_{\text{leak}}(\boldsymbol{x}_{\text{leak},l}, \hat{\gamma} t^{n+1}; b_l^n) - \sum_{\alpha=c,w} \left[\pi r^2_{\text{leak}} k_{l-} \lambda^n_{\alpha,\text{leak},l-} \times \left(\frac{\bar{p}^{n+1}_{\text{leak},l} - \bar{p}^{n+1}_{\text{leak},l-1}}{D_{l-}} + \rho_\alpha g \right) \right] G_{\text{leak},l}(\boldsymbol{x}_{\text{leak}}, \hat{\gamma} t^{n+1}; b_l^n) \quad (10)$$

When eq 10 is written for all layers, and boundary conditions are applied to the top and bottom layers of the system, the result is a set of algebraic equations for the unknown pressures at the leaky well. The resulting matrix has a tri-diagonal structure and may be solved by standard solution methods. For the case of only two layers, the system simplifies accordingly.

Saturation Updates. Once eq 10 is solved for pressures, fluxes in the abandoned well are calculated using eq 3, and saturations in each vertical segment of the abandoned well are updated using eq 4. Mass that is transferred between layers is accounted for within each layer, using the radial solution procedures described earlier. In the injection well, the flux is calculated from the well into the formation and appropriate fluid mass is added to that layer. Updated phase mobilities are calculated in all vertical segments of the abandoned well, based on the updated values of saturations. With this information, the coefficients to be used in the next time step may be determined, and the time-stepping procedure continues to the next time step.

Notice that the saturations that are updated in this IMPES-like algorithm are only those in the abandoned well. The radial saturation profile in the injection formation is calculated analytically as part of the injection solution. Therefore, that saturation profile is not updated as part of the "explicit saturation" part of the IMPES routine. In this way our IMPES-like algorithm differs from the traditional IMPES calculations.

Numerical Results

In this section we present two sets of numerical results. The first shows the effects of finite boundaries, as compared to solutions on infinite spatial domains, and also shows how the "upconing parameter" $b_{\max}$ affects the solutions. The second is a comparison between a series of semianalytical solutions and the corresponding solutions from numerical simulations using an industry-standard code. We consider a range of solutions and use them to show how leakage rate influences the upconing effect at the leaky well and to show the sensitivity of a representative solution to density and viscosity changes due to pressure changes.

The first example models CO_2 injection into a hypothetical formation with parameters characteristic of the Viking Formation of the Alberta basin in Canada (*16*, *33*). The injection rate is taken from Test Problem 7 in ref *34* as 0.317 kg/s per meter well, which is an approximation to the injection rate into the Utsira formation. When converted to volume at in-situ conditions, using the appropriate pressure and temperature, the CO_2 injection rate is about 1600 m^3/yr. The system includes one leaky well, located at a distance of slightly less than 1 km from the injection well. The leaky well perforates the impermeable aquiclude above the injection formation, and extends into an overlying permeable formation. Both the injection formation and the overlying permeable formation are 30 m thick, with permeability of 20 milliDarcy and porosity of 15%. The intervening aquiclude, which separates the two permeable formations, is 100 m thick and is impermeable. Top and bottom boundaries are impermeable. The leaky well is assigned a range of effective permeability values, from 100 milliDarcy to 10 Darcy. Table 1 provides all relevant parameters for these simulations. These data correspond to a basin with a relatively high geothermal gradient and a depth of approximately 3 km.

TABLE 1. Parameters Used in Simulation Study

CO_2 viscosity	0.0395 mPa·s
CO_2 density	479 kg/m^3
brine viscosity	0.2535 mPa·s
brine density	1045 kg/m^3
aquifer permeability	20 milliDarcy
aquifer thickness	30 m
leaky well permeability	1 Darcy
leaky well radius	14.1 cm
leaky well length	100 m
injection rate	1600 m^3/d
distance between wells	953 m
area of simulation domain	125.44 km^2

Figure 5 shows the semianalytical solution for CO_2 leakage in the leaky well as a function of time, where the leakage rate is expressed as a percent of the injection rate. The curves labeled "infinite" correspond to the solutions calculated on a domain with infinite boundaries, meaning the outer boundary is allowed to continue to expand indefinitely. The other three sets of curves show the effects of a finite boundary of fixed pressure on the CO_2 leakage rate. These curves were generated using the expanding outer boundary as described above, until the fixed outer boundary distance was reached, at which time the outer boundary was held fixed. The solid lines represent solutions calculated with $b_{\max}$ set to zero, so that the saturation in the well is set equal to one as soon as the CO_2 front arrives at the well ($b_{\max} = 0$ in eq 4). This instantaneous saturation of the well results in the sharp increase of leakage rate with time, as seen in Figure 5. The corresponding dashed lines show the solutions for the case of $b_{\max} = 0.15B$. For these cases the saturation increases linearly in the leaky well, from zero when $b = 0$ to one when $b = b_{\max}$. The effect of this extended period of saturation build-up is to produce a more gradual rise in CO_2 leakage, during which both CO_2 and brine flow in the leaky well. This represents the effect of upconing at the leaky well. In all of the solutions, the overall effect of the finite boundary is to limit the pressure build-up in the injection formation and therefore reduce the leakage rate as compared to the infinite aquifer. In addition, the rate of leakage decreases gradually in the finite-boundary cases at later times, while this leakage decrease is not observed in the infinite case. This gradual decrease is due to the finite-domain effects on the gradients in the upper permeable formation. Clearly the infinite case is the most conservative in terms of an estimate of the maximum leakage rate. In addition, we note that the curves plotted for each boundary condition show both the upper and lower bounds for the leakage estimates—because the leakage rate is low, the bounds fall essentially on top of one another and are indistinguishable on the graphs. Finally, we observe that the arrival time of the CO_2 front at the leaky well is unaffected by the position of the outer boundary. It is only the magnitude of the leakage that is influenced by the finite

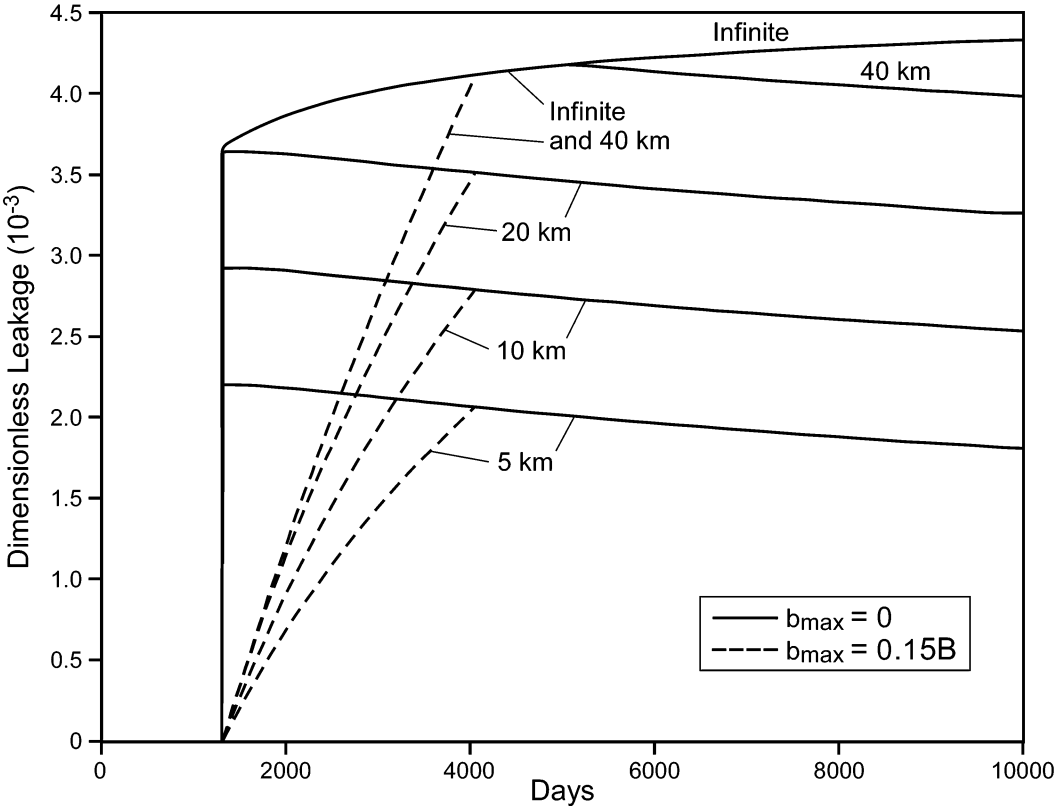

FIGURE 5. Semianalytical solutions showing leakage rate normalized by injection rate as a function of time, for infinite domain and for domains with finite outer boundaries. Outer boundary radii are indicated on the different curves.

location of the outer boundary. Notice that prior to the arrival of the CO_2 front, brine leaks out of the well, but its leakage rate is not shown in Figure 5.

For the second set of results, we have used the simulator Eclipse (*30*) to generate results to compare against results from the semianalytical method. The domain used is 11.2 km in both the x and y directions, with the z direction covering the two 30-m-thick aquifers and the 100-m-thick intervening impermeable aquitard. The leaky well is represented by a grid cell that is 0.25 m wide in the x and y directions and extends the entire vertical length of the domain. Notice that the cross-sectional area of the well is identical to the area assigned to the leaky well in the semianalytical solution. The injection well is located in the center of the (x,y) domain. A total of 16 900 grid cells (130 × 130) were used in the horizontal plane, with refinement around the leaky well, and 25 grid cells were used in the vertical direction, giving a total number of 422 500 grid cells. Further refinement did not produce significant changes in the numerical solution. The outer boundary was set as a fixed pressure, equal to the initial pressure, and the leakage of CO_2 into the upper permeable formation was monitored. Top and bottom boundaries were set as impermeable. We have run Eclipse with an assumption of constant density and viscosity, and with pressure dependence for both the density and viscosity. In addition, we have simulated three different effective permeability values in the leaky well: 0.1, 1, and 10 Darcy. For each of the cases, we have used a fitted value of b_{max} in the semianalytical solution and assumed constant values of density and viscosity based on the initial pressure.

Regarding simulation results, consider first the curves corresponding to the leaky-well permeability of 1 Darcy (Figure 6b). Four solutions are shown for this case: the semianalytical solution with $b_{max} = 0$ and $b_{max} = 0.15B$, the constant-density and constant-viscosity numerical simulations, and the pressure-dependent density and viscosity simulations. The density and viscosity equations of state were taken to correspond with Span and Wagner (*35*). For all of the solutions, the maximum leakage rate is about 0.25% of the injection rate. The semianalytical solution using a factor of $b_{max} = 0.15B$ shows good agreement with the numerical results. The two numerical results are close to one another, indicating that variations in density and viscosity caused by pressure changes play a secondary role in these solutions. The wiggles in the variable density and viscosity case appear to be small numerical instabilities in the Eclipse code. Notice that the long-time leakage rates are all very close to one another and that overall the solutions match well.

The results for the lowest well permeability also show a good match between the Eclipse simulations and the semianalytical solution, which in this case used a factor $b_{max} = 0.05B$. The smaller factor is consistent with the observation that for this lower leakage rate—about 0.025% of the injection rate—the upconing at the leaky well is weaker and therefore the period of two-fluid flow in the well is shortened considerably. Finally, for the highest permeability in the leaky well, 10 Darcy, we see a dramatic increase in the two-fluid flow period. That is manifested by the much slower rise in the CO_2 leakage rate. The semianalytical solution that provides a good match to the numerical simulation uses a values of $b_{max} = 0.5B$ For comparison, the case of $b_{max} = 0$ is also shown on the graph. That solution, which ignores upconing in the vicinity of the leaky well, identifies the maximum leakage rate, which is about 2% of the injection rate. That solution also shows a slight difference between the upper and lower bounds for leakage, which is the first time this difference has become apparent in the results. Overall, this result shows the importance of upconing at the leaky well and also shows the sensitivity of the maximum leakage rate to the characteristics of the well.

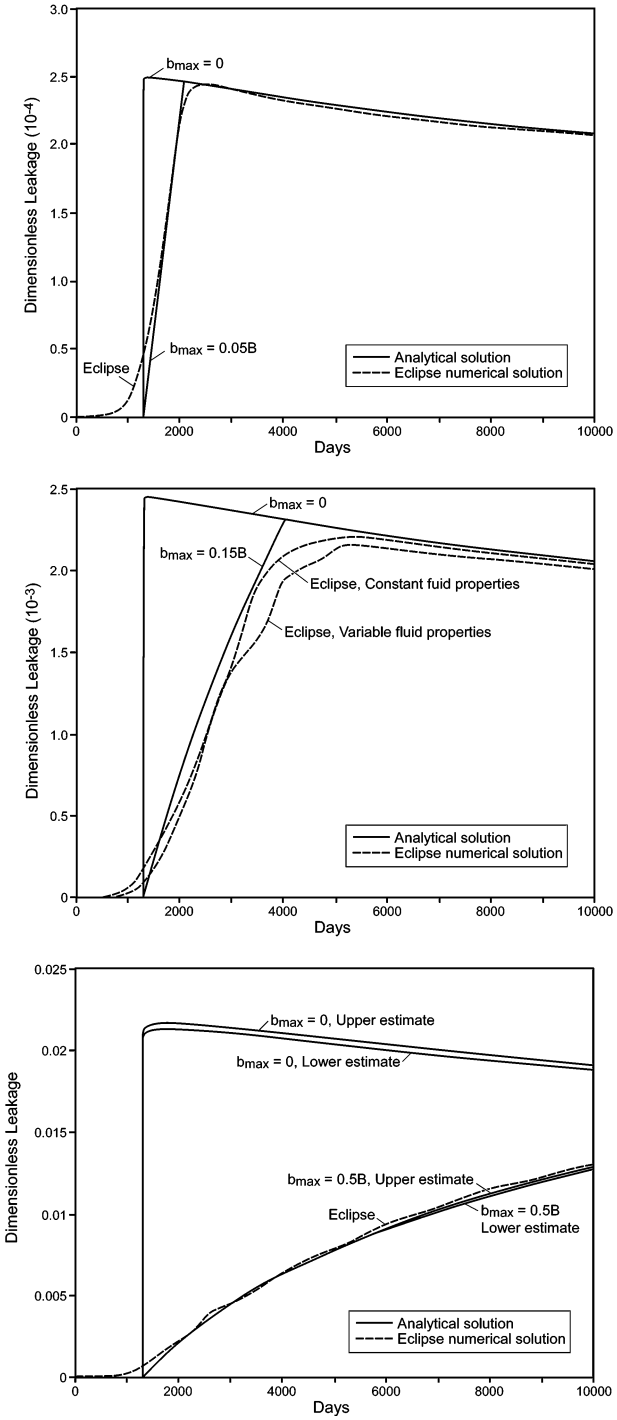

FIGURE 6. (a) Semianalytical and numerical solutions for well permeability of 0.1 Darcy. (b) Semianalytical and numerical solutions for well permeability of 1 Darcy. (c) Semianalytical and numerical solutions for well permeability of 10 Darcy.

Discussion

The semianalytical approach presented herein can simulate injection of CO_2 into a deep saline aquifer, with leakage along an abandoned well into an overlying aquifer. The solutions are easy to compute and very efficient, and for the cases we have examined they produce results that are close to the results from a full numerical simulator for two-fluid flow. These solutions provide insights into how the system behaves, in particular showing the influence of finite boundaries and the important effects of upconing in the vicinity of the leaky well.

While the semianalytical model is simple and efficient, and captures essential physics of the problem, like any analytical solution it is restricted by several important assumptions. All formations are assumed to be horizontal and of constant thickness. The formations are assumed to be homogeneous, and the intervening caprock layers are assumed to be impermeable. Density and viscosity are assumed constant, although each could be allowed to vary from one formation to the next, while remaining constant within any given formation. We have also assumed that capillary effects are small, we have set residual saturations to zero, and we have ignored mass transfer between phases. Below we comment on these assumptions, and speculate about how many of them can be relaxed in the context of an analytical framework.

The assumptions of horizontal layering, constant thickness, and homogeneity of materials within a given layer, are difficult assumptions to overcome. However, for practical purposes, it is often reasonable to make these assumptions in the vicinity of injection or pumping operations, or in cases with a general lack of resolved structural data on which to base a more detailed model. The assumption of constant density and viscosity appears to be reasonable for many ranges of pressure and temperature in the supercritical region of the CO_2 phase space. As we argue in the paper, when temperature and pressure are both near the critical point, then the dependence on pressure (and temperature) can become significant. For the cases of compressible CO_2, with viscosity also changing as a function of pressure, it appears that an extension of analytical methods based on similarity solutions can be derived which includes both density and viscosity variability as a function of pressure. We are currently working on these kinds of solutions. And, as was noted earlier, we already have a formulation in which density and viscosity can be varied between formations, while remaining constant within a given formation. Therefore the assumptions on density and viscosity do not appear to be restrictive. While we have chosen to implement the solution without residual saturation, it is not difficult to include it in the solution, while still assuming a sharp interface for the CO_2 invasion. Once residual saturation is included in the volume calculations, then we could also include equilibrium partitioning (dissolution) of CO_2 into the aqueous phase. We could also include water evaporation into the CO_2 phase. These processes are important to the geochemical nature of the fluids and therefore can be very important for predictions of degradation of well materials like well cements. However, because the amount that dissolves or evaporates is at most a few percent by volume, the effect is not large in terms of the overall movement of the CO_2 plume and its subsequent leakage. Therefore, we have options in the model formulation, and, through these options, we can include a reasonable representation of phase exchange between the two fluids. Capillary effects could influence the solution in at least three ways. First, capillary exclusion could keep the CO_2 from invading fine-grained materials such as the caprock. Because we assume the caprock has zero permeability, capillary exclusion is not relevant in this specific context. Second, it can spread the invading front via capillary diffusion. The effects of that action are usually small relative to the dominant advection process and therefore are not likely to produce significant changes to the solution, although they could become significant at large radial distances when the flow velocity becomes relatively small. Third, capillary exclusion can act on CO_2 in the leaky well to exclude it from entering the formation(s) along the leaky well due to entry pressure. The entry pressures could be large in the low-permeability layer but would be smaller in the more permeable layers. This kind of capillary entry effect could be included in the semianalytical model through modification of the perme-

ability at the well-formation interface, based on simple testing of the current pressure against the entry pressure. We have not included this feature in the current model.

The only fitting parameter in the model is the parameter b_{max}. This parameter captures the upconing behavior in the vicinity of the leaky well. The results of Figure 6 show that this parameter is a function of the flow rate in the well. One option to characterize this parameter is to run a number of simulations and determine an empirical fit as a function of flow rate. Another option, which we are pursuing, is to solve an equation to describe upconing in the vicinity of the well, as a two-fluid extension of the work done on saltwater intrusion and upconing in coastal aquifers (see, for example, ref *32*). That work appears to be promising, and we hope to have a derivation of the parameter b_{max}, or some equivalent parameter, based on these solutions.

An interesting observation from all of the solutions we have derived so far is that the upper and lower bounds appear to be very close to one another and only become apparent for large leakage rates. This implies that the solution is not sensitive to the multi-region approximation we use to derive the bounds, and that the overall approach is robust.

While the assumptions are restrictive, we believe that for many practical problems this solution procedure will not only provide important insights into the system behavior, but will also provide reliable and extremely efficient quantitative solutions. In the context of sensitivity analysis or Monte Carlo simulations, where many simulations need to be run in order to sample properly the parameter space, these solutions should prove to be very useful tools. We also believe this approach can be extended to include multiple wells by extension of the concepts in ref *20* to include two-fluid flows. We can also include more than two aquifers in the vertical sequence by implementing changes in density along the leaky wells, as discussed earlier. These kinds of solutions might also be coupled to more complex modules that describe details of fluid flow, component transport, and geochemical reactions within and along the leaky wells, with feedback involving changes in effective material properties. All of these require additions and extensions to the current solutions, but it appears that they can fit within the general framework we have outlined herein.

Acknowledgments

This work was supported in part by the Norwegian Research Council and Norsk Hydro through Grant 151400/210 to the University of Bergen, by BP and Ford Motor Company through the Carbon Mitigation Initiative at Princeton University, and by the Fulbright Fellowship program through a grant to M.A.C.

Literature Cited

(1) Kaya, Y. The role of CO_2 removal and disposal. *Energy Convers. Manage.* **1995**, *36*, 375−380.
(2) Bachu, S. Screening and ranking of sedimentary basins for sequestration of CO_2 in geological media. *Environ. Geol.* **2003**, *44*, 277−289.
(3) Jepma, C.; Munasinghe, M. *Climate Change Policy*; Cambridge University Press: New York, 1998; pp 331.
(4) Bajura, R. A. The role of carbon dioxide sequestration in the long-term energy future. In *Proceedings of the Fifth International Greenhouse Gas Technologies Conference*; Williams, D. J., Durie, R. A., McMullan, P., Paulson, C. A. J., Smith, A. Y., Eds.; CSIRO Publishing: Collingwood, Victoria, Australia, 2001; pp 52−58.
(5) Donaldson, E. C. Subsurface disposal of industrial waste in the United States. *Bur. Mines Inf. Circ.* **1964**, *No. 8212*, 32 pp.
(6) U.S. Environmental Protection Agency. *Report to Congress on Injection of Hazardous Waste*; EPA 570/9-85-003; Office of Drinking Water: Washington, DC, 1985.
(7) Moritis, G. CO_2 sequestration adds new dimension to oil, gas production. *Oil Gas J.* **2003**, *100* (15), 43−47.
(8) Bachu, S.; Haug, K.; Michael, K.; Buschkehle, B. E.; Adams, J. J. Deep injection of acid gas in western Canada. In *Proceedings of the Second International Symposium on Underground Injection Science and Technology*, October 23−25, 2003; Tsang, C.-F., Apps, J. A., Eds.; Berkeley, CA, in press.
(9) Torp, T. A.; Gale, J. Demonstrating storage of CO_2 in geological reservoirs: The Sleipner and SACS projects. *Energy* **2004**, *29* (9−10), 1361−1369.
(10) Bachu, S. Geological sequestration of anthropogenic carbon dioxide: applicability and current issues. In *Geological Perspectives of Global Climate Change*; Gerhard, L., Harrison, W. E., Hanson, B. M., Eds.; AAPG Studies in Geology 47; American Association of Petroleum Geologists: Tulsa, OK, 2001; pp 285−304.
(11) Celia, M. A.; Bachu, S. Geological sequestration of CO_2: is leakage unavoidable and acceptable? In *Proceedings of the Sixth International Greenhouse Gas Technologies Conference*, Kyoto, Japan, October 1−5, 2002; Gale, J., Kaya, Y., Eds.; Pergamon: 2003; Vol. I, pp 477−482.
(12) Farrar, C. D.; Sorey, M. L.; Evans, W. C.; Howle, J. F.; Kerr, B. D.; Kennedy, B. M.; King, C.-Y.; Southon, J. R. Forest-killing diffuse CO_2 emission at Mammoth Mountain as a sign of magmatic unrest. *Nature* **1995**, *376*, 675−678.
(13) Hepple, R. P.; Benson, S. M. Implications of surface seepage on the effectiveness of geologic storage of carbon dioxide as a climate change mitigation strategy. In *Proceedings of the Sixth International Greenhouse Gas Technologies Conference*, Kyoto, Japan, October 1−5, 2002; Gale, J., Kaya, Y., Eds.; Pergamon: 2003; Vol. I, pp 261−266.
(14) Pacala, S. W. Global constraints on reservoir leakage. In *Proceedings of the Sixth International Greenhouse Gas Technologies Conference*, Kyoto, Japan, October 1−5, 2002; Gale, J., Kaya, Y., Eds.; Pergamon: 2003; Vol. I, pp 267−272,
(15) Intergovernmental Panel on Climate Change. *Climate Change 1995: The Science of Climate Change*; Cambridge University Press: Cambridge, U.K., 1996; p 572.
(16) Gasda, S. E.; Bachu, S.; Celia, M. A. Spatial characterization of the location of potentially leaky wells penetrating a deep saline aquifer in a mature sedimentary basin. *Environ. Geol.* **2004**, *46*, 707−720.
(17) Lindeberg, E. Vertical convection in an aquifer column under a gas cap of CO_2, *Energy Convers. Manage.* **1997**, *38*, S229−S234.
(18) Xu, T.; Apps, J. A.; Preuss, K. Reactive geochemical transport simulation to study mineral trapping for CO_2 disposal in deep arenaceous formations. *J. Geophys. Res.* **2003**, *108* (B2), 2071, doi: 10.1029/2002JB001979.
(19) Nordbotten, J. M.; Celia, M. A.; Bachu, S. Injection and storage of CO_2 in Deep saline aquifers: Analytical solution for CO_2 plume evolution during injection. *Transp. Porous Media* (in press).
(20) Nordbotten, J. M.; Celia, M. A.; Bachu, S. Analytical solutions for leakage rates through abandoned wells. *Water Resour. Res.* **2004**, *40*, W04204.
(21) Klusman, R. W. Evaluation of leakage potential from a carbon dioxide EOR/sequestration project. *Energy Convers. Manage.* **2003**, *44*, 1921−1940.
(22) Law, D. H.-S.; Bachu, S. Hydrogeological and numerical analysis of CO_2 disposal in deep aquifers in the Alberta sedimentary basin. *Energy Convers. Manage.* **1996**, *37*, 1167−1174.
(23) Lindeberg, E. Escape of CO_2 from aquifers, *Energy Convers. Manage.* **1997**, *38S*, S235−S240.
(24) McPherson, B. J. O. L.; Cole, B. S. Multiphase CO_2 flow, transport and sequestration in the Powder River Basin, Wyoming, U.S.A. *J. Geochem. Explor.* **2000**, *69*−*70*, 65−70.
(25) Saripalli, P.; McGrail, P. Semi-analytical approaches to modeling deep well injection of CO_2 for geological sequestration. *Energy Convers. Manage.* **2002**, *43*, 185−198.
(26) Blunt, M.; King, P. Relative permeabilities from two- and three-dimensional pore-scale network modeling. *Transp. Porous Media* **1991**, *6*, 407.
(27) Buckley, S. E.; Leverett, M. C. Mechanisms of fluid displacement in sands. *Trans. AIME* **1942**, *146*, 107−116.
(28) Dietz, D. N. A theoretical approach to the problem of encroaching and bypassing edge water. *Proc. K. Acad. Wetenschappen* **1953**, *B56*, 83−92.
(29) Yortsos, Y. C. A theoretical analysis of vertical flow equilibrium. *Transp. Porous Media* **1995**, *18* (2), 107−129.
(30) Schlumberger Information Systems. Eclipse technical description, 2002.
(31) van Lookeren, J. Calculation methods for linear and radial steam flow in oil reservoirs. *SPE* **1977**, *No. 6788*.
(32) Bower, J. W.; Motz, L. H.; Durden, D. W. Analytical solution for determining the critical condition of saltwater upconing in a leaky artesian aquifer. *J. Hydrol.* **1999**, *221*, 43−54.

(33) Bachu, S.; Adams, J. J. Sequestration of CO_2 in geological media in response to climate change: Capacity of deep saline aquifers to sequester CO_2 in solution. *Energy Convers. Manage.* **2003**, *44*, 3151−3175.

(34) Pruess, K.; García, J.; Kovscek, T.; Oldenburg, C.; Rutqvist, J.; Steefel, C. Xu, T. *Intercomparison of numerical simulation codes for geologic disposal of CO_2*; LBNL-51813; Lawrence Berkeley National Laboratory Report: Berkeley, CA, 2002.

(35) Span, R.; Wagner, W. A new equation of state for carbon dioxide covering the fluid region from the triple-point temperature to 100 K at pressures up to 800 MPa. *J. Phys. Chem. Ref. Data* **1996**, *25* (6), 1509−1596.

Received for review December 2, 2003. Revised manuscript received September 21, 2004. Accepted October 8, 2004.

ES035338I